Journal of Marine Science and Technology

Volume 23 | Issue 5 Article 22

A NUMERICAL STUDY OF LIQUID TANK AND STRUCTURE INTERACTION

Bang-Fuh Chen
Department of Marine Environment and Engineering, National Sun Yat-sen University, Kaohsiung, Taiwan, R.O.C., chenbf@mail.nsysu.edu.tw

Shih-ming Huang
Department of Marine Environment and Engineering, National Sun Yat-sen University, Kaohsiung, Taiwan, R.O.C.

Recommended Citation
Chen, Bang-Fuh and Huang, Shih-ming (2015) "A NUMERICAL STUDY OF LIQUID TANK AND STRUCTURE INTERACTION," *Journal of Marine Science and Technology*: Vol. 23: Iss. 5, Article 22.
DOI: 10.6119/JMST-013-0815-1
Available at: https://jmstt.ntou.edu.tw/journal/vol23/iss5/22

A NUMERICAL STUDY OF LIQUID TANK AND STRUCTURE INTERACTION

Acknowledgements

The study was supported by the National Science Council of ROC under grants NSC 97-2221-E-110-087 and NSC 98-3114-P-110-001.

Journal of Marine Science and Technology, Vol. 23, No. 5, pp. 781-791 (2015)
DOI: 10.6119/JMST-013-0815-1

A NUMERICAL STUDY OF LIQUID TANK AND STRUCTURE INTERACTION

Bang-Fuh Chen and Shih-ming Huang

Key words: fully nonlinear free-surface condition, sloshing liquid, tuned liquid damper, fluid-structure interaction, seismic reduction control.

ABSTRACT

A time-independent finite difference method was used to solve for a fully nonlinear sloshing fluid in a tank mounted on a structure. The interaction between the sloshing fluid and the dynamic response of the structure was investigated. The dynamic response of the structure was calculated using the fourth-order Runge-Kutta method, and the numerical model was extensively validated through comprehensive data comparisons. The tank was tuned to an appropriate depth to length ratio and was used as a tuned liquid damper. Several cases, including large and small structures, were studied. In addition, a vibration control analysis of the tank-structure system in a real earthquake scenario is described in this paper. Vibration control was tested in terms of reduction in the dynamic response of the structure and reduction in the maximum energy development in the tank-structure system during excitation. The response of the tank-structure system was sensitive to the excitation frequency and water depth in the fluid tank.

I. INTRODUCTION

Free-surface sloshing in a moving container is associated with various engineering problems, such as those associated with tankers on highways, liquid oscillations in large storage tanks caused by earthquakes, sloshing of liquid cargo in ocean-going vessels, and the motion of liquid fuel in aircraft and spacecraft. Partially filled tanks are prone to violent sloshing under certain conditions, particularly at near-resonant excitation. The large amplitude movement of a liquid can create high impact pressures on the tank walls, which in turn can cause structural damage and even create moments that affect the stability of the vehicles carrying the containers.

Sloshing fluid inside a liquid tank subjected to excitation has been intensively studied for decades. The earlier analyses were based on linear, weakly nonlinear, and inviscid conditions (Faltinsen, 1978; Nakayama and Washizu, 1981; Chen and Chiang, 1999). In recent years, studies have reported on fully nonlinear free-surface boundary conditions, complete primitive Navier-Stokes equations, and fluid viscosity (Okamoto and Kawahara, 1990; Koh et al., 1994; Armenio and Rocca, 1996; Kim, 2001; Fradensen, 2004; Chen and Nokes, 2005). This study focused on the resonant sloshing phenomenon and the coupling effects of surge, sway, and heave motions.

New types of cost-efficient dampers that can mitigate earthquake- and wind-induced vibrations of tall buildings and long-span bridges have been studied for many years. The most commonly used auxiliary damping device is the tuned mass damper (TMD), which consists of a mass attached to a building through a spring and a dashpot. TMDs have been implemented in condo towers in San Francisco and the Citicorp building in New York City. In addition to a TMD, a liquid tank is frequently used as a tuned liquid damper (TLD) to reduce possible violent oscillations of structures (Sun et al., 1992; Reed et al., 1998; Banerji et al., 2000). The sloshing effect of a fluid in a tank is tuned to produce a desired reaction for reducing the vibration of the structures attached to the liquid tank. One of the most commonly used TLDs is the tuned liquid column damper, which consists of a U-shaped tube; the motion of the fluid oscillating in the column counteracts the force acting on the structure. Innovative liquid dampers have been applied in ship and satellite stabilization and more recently in building stabilization.

TLDs can be easily installed in various structures, and the installation and maintenance fees are considerably cheaper than those of TMDs. However, a resonant sloshing wave in a TLD cannot be quickly returned to a calm state after stopping the excitation (Fujino, 1988). Gardarsson (2001) indicated that inclined tank walls can reduce the effects of sloshing forces on the vibration of structures.

A linear theory proposed by Lepelletier and Raichlen (1988) and numerical methods proposed by Nomura (1994) and Yamamoto and Kawahara (1999) are used in TLD analyses. Kareem (1999) used a boundary element method and studied the effects of the number of circular cylinder TLD tanks on the reduction rate of vibration of structures. Frandsen (2004) reported a finite difference method to study the characteristic

Paper submitted 03/27/12; revised 05/02/13; accepted 08/15/13. *Author for correspondence: Bang-Fuh Chen (e-mail: chenbf@mail.nsysu.edu.tw).*
Department of Marine Environment and Engineering, National Sun Yat-sen University, Kaohsiung, Taiwan, R.O.C.

frequencies that can effectively reduce the vibration of structures. In the study by Frandsen, a rectangular liquid tank mounted on the surface of a structure was used. Frandsen reported that two characteristic frequencies were associated with the reduction of the vibration of the structures. When the excitation frequency was close to the first fundamental frequency of the tank, the beating response occurred, and the interaction between the sloshing tank and structure base was the strongest. In Frandsen's analysis, the motion of the tank-structure system was restricted to the x direction. However, earthquake motion is simultaneously excited in the x and y directions.

In this study, a tank-structure system similar to that reported by Frandsen (2004) was adopted, a time-independent finite difference method (Chen and Nokes, 2005) was used to evaluate the response of a sloshing fluid in a tank, and the Runge-Kutta method was used to calculate the dynamic response of the spring-mounted base structure system. The mathematical formulation and numerical scheme are detailed in Section 2. Section 3 describes the results and discussion, and Section 4 presents the conclusions.

II. MATHEMATICAL FORMULATION OF A SLOSHING FLUID IN A TANK

In this study, the tank motion is represented using a coordinate system (Fig. 1). The Euler equations, including surge and heave motions, can be written as (Chen and Chiang, 1999):

$$\frac{\partial u}{\partial t}+u\frac{\partial u}{\partial x}+w\frac{\partial u}{\partial z}=-\frac{1}{\rho}\frac{\partial p}{\partial x}-\ddot{x}_c \tag{1}$$

$$\frac{\partial w}{\partial t}+u\frac{\partial w}{\partial x}+w\frac{\partial w}{\partial z}=-g-\frac{1}{\rho}\frac{\partial p}{\partial z}-\ddot{z}_c \tag{2}$$

where u and w are the velocity components of the fluid in the x and z directions, respectively, $\ddot{x}_c$ and $\ddot{z}_c$ are the corresponding ground acceleration components, respectively, p is the pressure, ρ is the fluid density, and g is the gravitational acceleration. The continuity equation for the incompressible flow can be expressed as

$$\frac{\partial u}{\partial x}+\frac{\partial w}{\partial z}=0 \tag{3}$$

The kinematic boundary condition on a free surface is

$$\frac{\partial h}{\partial t}+u\frac{\partial h}{\partial x}=w \tag{4}$$

Dynamic free-surface conditions were used to calculate the dynamic pressure (Chen, 1999):

$$p_0=\rho g(h-d_0) \tag{5}$$

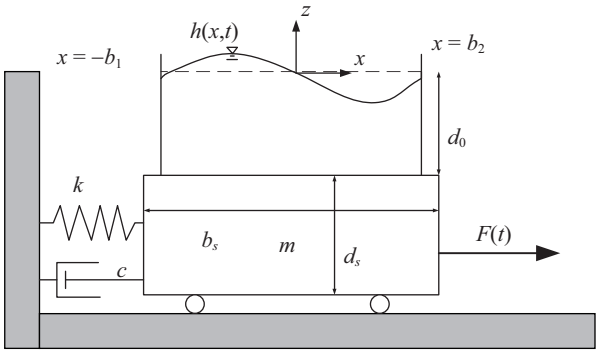

Fig. 1. The definition sketch of tank-base structure system.

Summing the partial differentiation of Eqs. (1) and (2) with respect to the x and z directions yields

$$\nabla^2 p=-\rho\frac{\partial}{\partial x}(u\frac{\partial u}{\partial x}+w\frac{\partial u}{\partial z})-\rho\frac{\partial}{\partial z}(u\frac{\partial w}{\partial x}+w\frac{\partial w}{\partial z}) \tag{6}$$

1. Coordinate Transformation and Dimensionless Equations

Instead of using a boundary-fitted coordinate system, we used simple mapping functions to remove the time-varying boundary of the fluid domain. The mapping functions and the related finite difference scheme have been successfully used in various computational fluid dynamic studies (Chen, 1997; 1999). The irregular tank walls and tank bottom were mapped onto a square domain by using appropriate coordinate transformations as follows (Chen, 1994):

$$x^*=\frac{x-b_1}{b_2-b_1} \tag{7}$$

and

$$z^*=1-\frac{z-d_0}{h(x,t)} \tag{8}$$

where the instantaneous water surface $h(x,t)$ is a single value function and is measured from the tank bottom, d_0 represents the vertical distance between still water surface and tank bottom, and b_1 and b_2 are horizontal distances from the z-axis to the left and right walls, respectively. According to Eqs. (7) and (8), the left wall, right wall, free surface, and tank bottom can be mapped onto $x^*=0$, $x^*=1$, $z^*=0$, and $z^*=1$, respectively. The main advantage of these transformations is that a nonrectangular and time-dependent flow field can be mapped onto a time-independent square domain. In this case, all time-dependent geometric and dynamic boundary conditions were included in the equations of motion along with the tank motion. The mapping functions neglect the possibility of overturning of the free surface. The coordinates (x^*, z^*) can be further

transformed so that the layers near the free surface, tank bottom, and tank wall are stretched by the following exponential functions:

$$X = \beta_1 + (x^* - \beta_1)e^{k_1 x^*(x^*-1)} \tag{9}$$

$$Z = \beta_2 + (z^* - \beta_2)e^{k_2 z^*(z^*-1)} \tag{10}$$

The constants k_2 and β_2 control the mesh sizes near the free surface and tank bottom, respectively, and the constants k_1 and β_1 map the irregular finite difference mesh sizes (Δx^*) near the tank wall onto the regular mesh sizes (ΔX) in the computational domain (X, Z). Thus, the geometry of the flow field and meshes in the computational domain (X-Z system) are time-independent throughout the computational analysis. The velocity components are normalized using the maximum horizontal ground velocity u_m, such as $U = u/u_m$ and $W = -w/u_m$. The pressure p is normalized using the hydrostatic pressure $\rho g d_0$ in which d_0 is the undisturbed fluid depth; that is, $P = p/\rho g d_0$. The dimensionless time is defined as $T = u_m t/d_0$. The instant fluid depth is normalized using d_0; that is, $H = h/d_0$, $X_c = x_c/B$, $Z_c = z_c/B$. B is the tank width.

Thus, using the aforementioned transformations and dimensionless variables, Eq. (1) can be expressed in a dimensionless form as follows:

$$\begin{aligned} &U_T + C_5C_7U_X + C_6C_8U_Z + C_1C_7UU_X + C_2C_8UU_Z \\ &+ C_3C_7WU_X + C_4C_8WU_Z \\ &= -\frac{1}{F^2}(C_1C_7P_X + C_2C_8P_Z) - X_{cTT} \end{aligned} \tag{11}$$

In Eq. (11), the Froude number F can be expressed as $F = \frac{u_0}{\sqrt{gd_0}}$.

In the aforementioned equations, $C_1 - C_{10}$ are the coefficients generated through coordinate transformations (Chen and Nokes, 2005) and U_T denotes a partial derivative of U with respect to dimensionless time; the other terms have similar meanings. Under fully nonlinear free-surface conditions, the kinematic free-surface condition is applied at the instantaneous free surface; that is, at $z = h - d_0$, the physical domain should consider the variation of the free surface, and the coefficients $C_1 - C_{10}$ related to the free surface should be updated iteratively.

2. Finite Difference Method

The numerical method based on a finite difference method is used in this study. Many finite difference and finite volume methods have been proposed for evaluating a free surface. The most commonly used schemes are SURF, Maker and Cell (MAC), and volume of flow (VOF) methods. The SURF scheme assumes a single-value surface profile and can handle a uniform representation of large free surface waves and overturning inception. The widely adopted MAC method is a Largrangian concept and can manage overturning waves and re-entry inception using a simple logic. The VOF method is the most frequently used and tracks the volume occupied by the fluid rather than the free surface. These aforementioned methods appropriately calculate the instant free-surface displacement. However, they require complicated computer programming for treating the time-varied free-surface boundary and updating computational meshes. Alternatively, in this study, the time-varied free-surface boundary was transformed into a time-independent free surface in the x^*–z^* domain, and boundary tracing was not required during calculations. A single-value height function was assumed and is evaluated by solving the kinematic free-surface conditions.

In a two-dimensional analysis, fluid flow is solved in a rectangular mesh network of the transformed domain. The staggered grid system is used in the analysis; that is, the pressure P is applied at the mesh center, and the velocity components U and V are set at $0.5\Delta X$ behind and $0.5\Delta Z$ above the center, respectively. The Crank-Nicholson iteration scheme and Gauss-Seidel Point successive over-relaxation iteration procedures were used to calculate the velocity and pressure, respectively. The advantages and disadvantages of the proposed method and detailed implicit iterative procedures and convergence criterion have been described by Chen and Nokes (2005).

3. Equations of Motion of Base Structures

The definition sketch of a tank-structure system is depicted in Fig. 1. A tank is mounted on top of a base structure by using a spring and a dashpot. The dynamic equations of motion of spring-mounted base structures can be written as

$$m\ddot{\delta}(t) + c\dot{\delta}(t) + k\delta(t) = F(t) + F_{\text{sloshing}}(t) \tag{12}$$

where m is the mass of the base structure; $\ddot{\delta}(t)$, $\dot{\delta}(t)$, $\delta(t)$ are the dynamic acceleration, velocity, and displacement of the structure, respectively; $F(t)$ is the exciting external force that is applied to the system; k is the spring stiffness; c is the damping coefficient; $F_{sloshing}(t)$ is the sloshing force that acts on the base structure; $h(x,t)$ is the water surface elevation; d_0 is the water depth; and d_s and b_s are the depth and length of the base structure, respectively. The fourth-order Runge-Kutta method was used to solve Eq. (12). The solved dynamic acceleration was used as the external forcing acting on the tank. The calculated sloshing force affects the exciting force acting on the base system, thus subsequently changing the dynamic response of the base structure and external forcing on the tank. Use of the Runge-Kutta fourth-order scheme for time marching necessitated three internal substep calculations, including those of the respective boundary conditions for free-surface and body boundaries. The simulated problem is an interaction problem of a sloshing fluid and base structure.

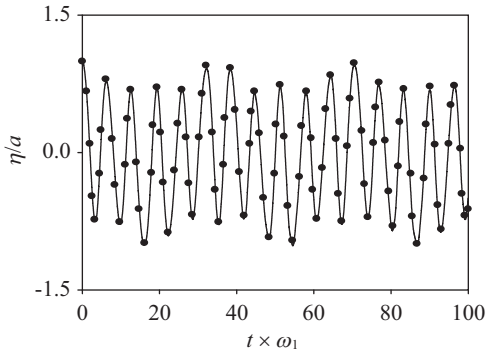

Fig. 2. The comparison of the surface elevation at left wall of vertical excited tank obtained by present study (solid line) and Frandsen (2004) (symbol). η: the sloshing displacement at left wall; a: initial wave amplitude 0.00097 m, $\omega_1 = 3.758$ (first order sloshing wave mode).

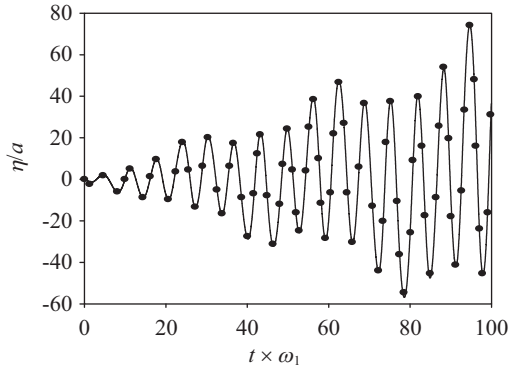

Fig. 3. The comparison of the surface elevation at left wall of vertical excited tank obtained by present study (solid line) and Frandsen (2004) (symbol). η: the sloshing displacement at left wall; a: initial wave amplitude 0.00097m, ω_1: 3.758 (first order sloshing mode), ω_v: 0.798 * ω_1, ω_h: 0.98 * ω_1, k_v: 0.5 , k_h: 0.0014.

III. RESULTS AND DISCUSSION

The calculated results were validated through several data comparisons. We first simulated the sloshing of a fluid-filled tank with a vertical harmonic acceleration (0.5 g) with an excitation period of 2.99 s. The initial free surface of the fluid in the tank is $\zeta(0, x) = a\cos(\kappa x)$, where a is the initial amplitude of the surface wave, κ is the wave number, and the wave length is 2 m. Fig. 2 shows the sloshing elevation at the left wall of the tank along with the results obtained by Frandsen (2004); as shown, our results are consistent with those reported by Frandsen.

For two-dimensional excitation, the tank was horizontally (0.0014 g) and vertically (0.5 g) accelerated at excitation periods of 0.98 and 0.798 times the first fundamental period of the fluid in the tank, respectively. Fig. 3 illustrates the free-surface elevation at the left wall. The solid line and symbol plot the results of our study and those reported by Frandsen (2004), respectively, which as can be seen are consistent.

Table 1 The lowest sloshing frequencies of a tank with various liquid depths 5.

d_0 (b = 2 m)	0.3	0.4	0.5	0.6	0.7	0.8	0.9
ω_o	20601	2.929	3.179	3.368	3.512	3.619	3.699

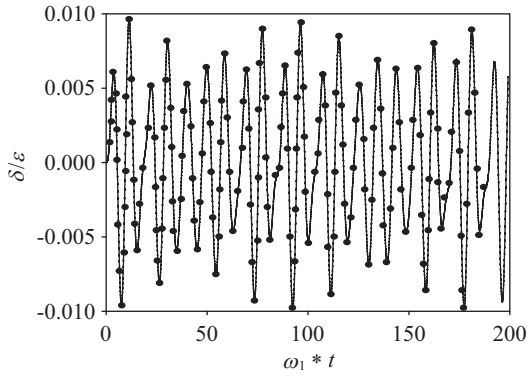

Fig. 4. The comparison of the dynamic displacement of the tank-structure between present study (solid line) and Frandsen (2005) (solid symbol) (ε = 0.102, Tank Length = 2 m, Depth = 1 m, β = 0.665, ω_1 = 3.758, mesh 80 * 40).

1. Tank-Structure Interaction

In this section, the parameters used by Frandsen (2005) were adopted. The ratio of the depth of the fluid to the length of tank is d_0/b; the mass ratio is μ; the tuning ratio is $\Omega_n^T = \omega_n/\omega_o$, where ω_n is the n^{th} fundamental frequency of the fluid in the tank; and ω_o is the natural frequency of the structure system. The fundamental frequencies of the fluid in the tank at various fluid depths are listed in Table 1. We define the parameter $\beta = \omega_f/\omega_o$, where ω_f is the external forcing frequency. Two excitation frequencies were used: one was applied outside the resonant region ($\beta = 0.665$) and the other was applied at resonance (β = 0.968). The external forcing function is $F(t) = A_F\cos(\omega_f t)$, and the dimensionless forcing amplitude is $\varepsilon = A_F/(\rho g d_0^2)$.

Fig. 4 depicts the time history of the dynamic displacement of a tank-structure at a harmonic horizontal excitation with a dimensionless forcing amplitude $\varepsilon = 0.102$, frequency $\beta = 0.665$, d_0/b = 1/2, and $\mu = 0.01$. The solid line and solid symbol represent the numerical results of this study and those reported by Frandsen (2005), respectively. As can be seen, the results of this study are consistent with those reported by Frandsen (2005). Fig. 5 is a similar plot of the sloshing displacement at the left wall of the tank; the results of this study are consistent with those reported by Frandsen (2005).

For a near-resonant excitation, we increased the excitation frequency to $\beta = 0.968$. Figs. 6 and 7 present a comparison of the numerical results of this study and those of Frandsen (2005), which as can be seen are consistent.

2. Parametric Tests of Mesh Size and Time-Step Selection

We conducted several parametric tests to investigate the

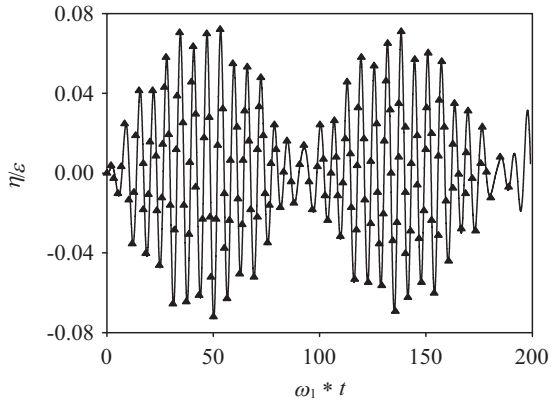

Fig. 5. The comparison of the sloshing displacement at left wall of the tank between present study (solid line) and Frandsen (2005) (solid symbol) (ε = 0.102 , tank length = 2 m, depth = 1 m, β = 0.665, ω_1 = 3.758, mesh 80 * 40).

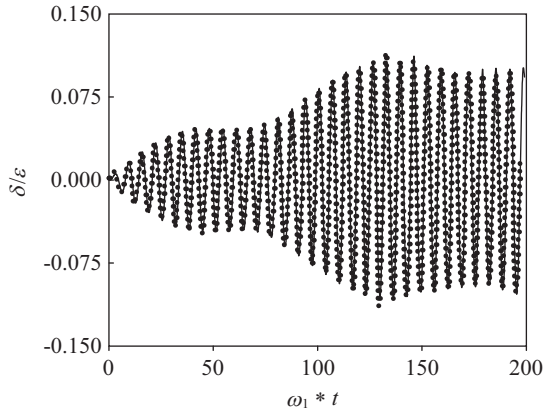

Fig. 6. The comparison of the dynamic displacement of the tank-structure between present study (solid line) and Frandsen (2005) (solid symbol) (ε = 0.102, tank length = 2 m, depth = 1 m, β = 0.968, ω_1 = 3.758).

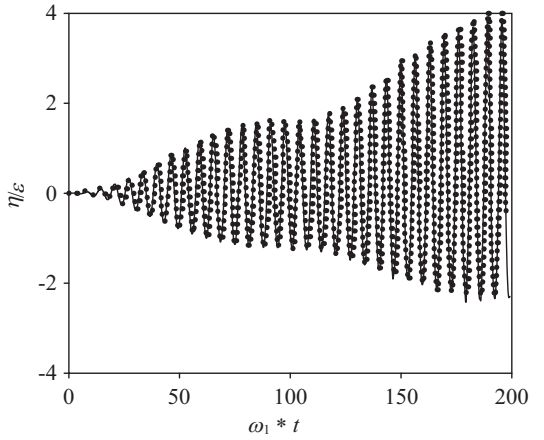

Fig. 7. The comparison of the sloshing displacement at left wall of the tank between present study (solid line) and Frandsen (2005) (solid symbol) (ε = 0.102, tank length = 2 m, depth = 1 m, β = 0.968 , ω_1 = 3.758).

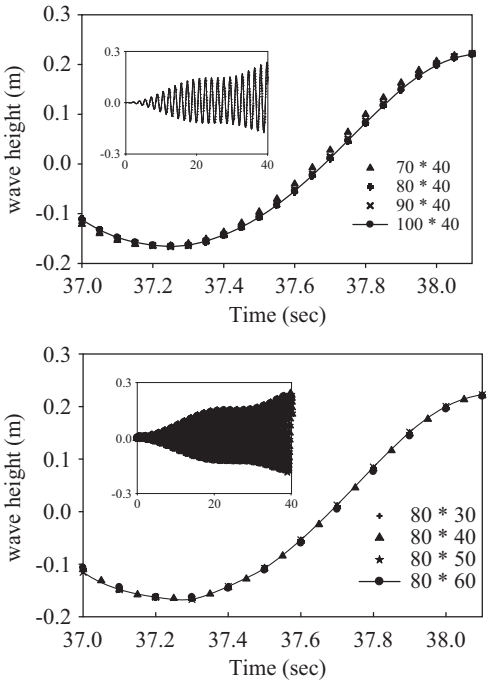

Fig. 8. The effects of mesh-size arrangement on sloshing displacement at left wall of the tank; the left plots are the results of various M with fixed N and the right plots are those of various N with fixed M. (d_0/b = 1/2 and μ = 0.01, β = 0.968).

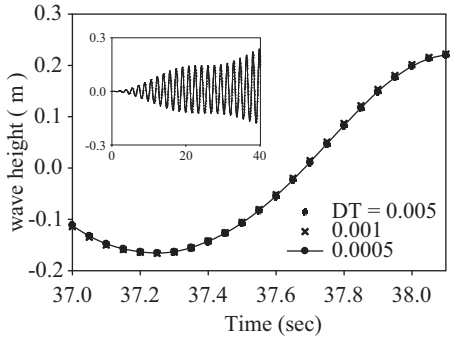

Fig. 9. The effects of time step selection on the sloshing displacement at the left wall of the tank, (d_0/b = 1/2 and μ = 0.01, β = 0.968).

effects of mesh size arrangement on the sloshing displacement at the left wall of the tank. The tank size was d_0/b = 1/2 and μ = 0.01. The forcing function was $F(t)$ = 1000 * sin($\omega_f t$), and the excitation frequency was β = 0.968. Fig. 8 shows the effects of mesh size arrangement on the sloshing displacement at the left wall of the tank. The left plots represent the results of various M (mesh number in the x direction) with fixed N (mesh number in the z direction), and the right plots represent the results of various N with fixed M. The results were invariant for mesh sizes smaller than M × N = 80 × 40 and were therefore used for simulations in this study. The time step used in the aforementioned simulation is ΔT = 0.001. The effects of the time step on the sloshing displacement are illustrated in Fig. 9. The sloshing displacements obtained using the current

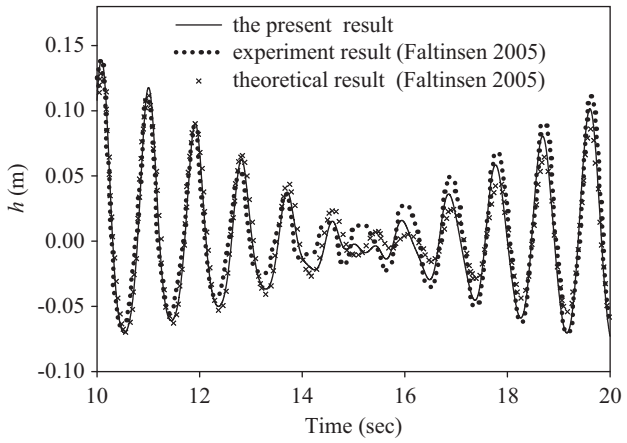

Fig. 10. The comparisons of liquid tank between experimental measurement, analytical results, and the present results of wave elevation at left wall, $d_0/b = 0.5$, $b = 1$ m, $\omega_f = 1.037\ \omega_1$.

numerical model at $\Delta T = 0.0005$, 0.001, and 0.005 were nearly the same, and therefore $\Delta T = 0.001$ was used for all simulations.

Using the selected mesh size and time step, Our simulation results are consistent with theoretical and experimental results reported by Faltinsen et al. (2005) for a sloshing fluid in a tank with $d_0/b = 0.5$ and $\omega_f = 1.037\ \omega_1$.

3. Vibration Control ($\mu = 0.01$: Large Structure; $\mu = 1/3$: Small Structure)

After extensive numerical validation, we used two descriptions to discuss the vibration control of a tank-structure system: the reduction in the maximum dynamic displacement of a structure and the reduction in the maximum energy developed in a tank-structure system. The term "maximum" indicates the peak value of the transient response, which is generally the highest response, occurring at the first beating because it is at near-resonant excitation. We simulated a tank-structure system with $\mu = 0.01$ and various water depths in the tank. Three cases ($d_0/b = 0.3$, 0.4, and 0.6) are reported in this paper. The structure weighs considerably more than does the water in the tank, and μ is assumed to be constant (0.01) at all water depths. Fig. 11 depicts the dynamic displacement of the structures with and without a tank mounted on it at a near-resonance excitation with $\beta = 0.968$ and $\varepsilon = 0.102$. The tank with $d_0/b = 0.4$ showed the maximum reduction in the dynamic response of the structure, and that with $d_0/b = 0.6$ enhanced the dynamic response of the structure.

The tank-structure systems described in previous studies were large structures with a small tank; the mass ratio of the tank to the structure in these studies was low (0.01), and the mass of the system was assumed to be invariant. We simulated a tank-structure system with a considerably high mass ratio of the tank to the structure ($\mu = 1/3$) and $d_0/b = 0.15$. In this study, the forcing amplitude was a constant (30 N) at various excitation frequencies, and the maximum energy development in the tank-structure system was studied. Fig. 12 shows the plot of the time histories of the structure displacement, water

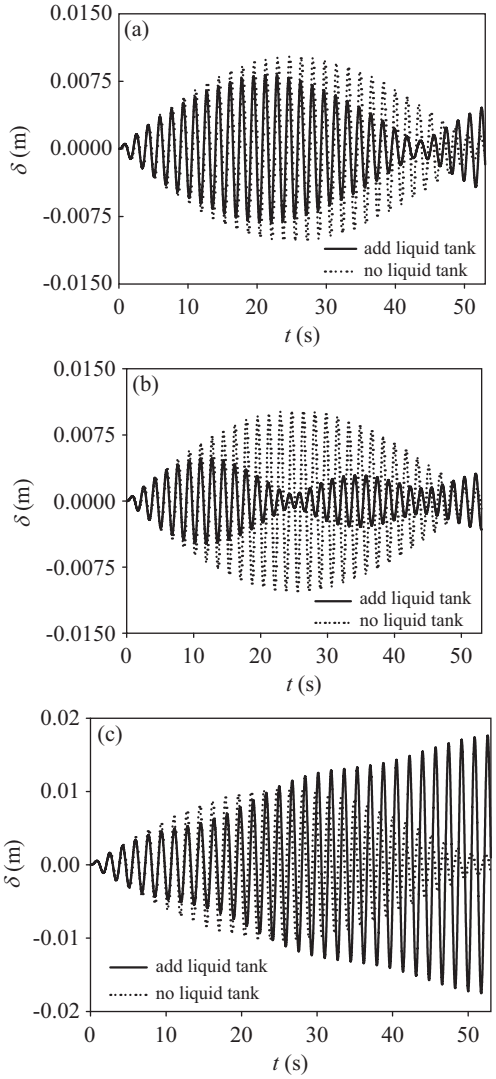

Fig. 11. The dynamic response of structures with and without tank-mounted; $\beta = 0.968$ $\mu = 0.01$ and $\varepsilon = 0.102$. (water depth = (a): 0.6 m, (b): 0.8 m, (c): 1.2 m).

elevation at the left wall, and energy built in the system at various excitation frequencies. Both dynamic displacement of the structure and sloshing displacement of water at the left wall of the tank were the largest at $\beta = 0.9$, followed by at $\beta = 0.6$. Fig. 13(a) depicts the energies developed in the tank-structure system at various excitation frequencies. Two peaks corresponding to $\beta = 0.6$ and 0.9 were observed, implying that the energy development in the system is related to the dynamic displacement and sloshing displacement of the fluid. Furthermore, we calculated the maximum energy production in the structure system without a tank mounted on it; Fig. 13(b) shows the corresponding energy development. As expected, a peak was observed at $\beta = 1$. According to Fig. 13(a) and (b), the resonance frequency of the tank-structure system shifted to the left, and the maximum peak energy decreased considerably. Therefore, the tuned tank-structure system for vibration control is applicable to a small-structure system.

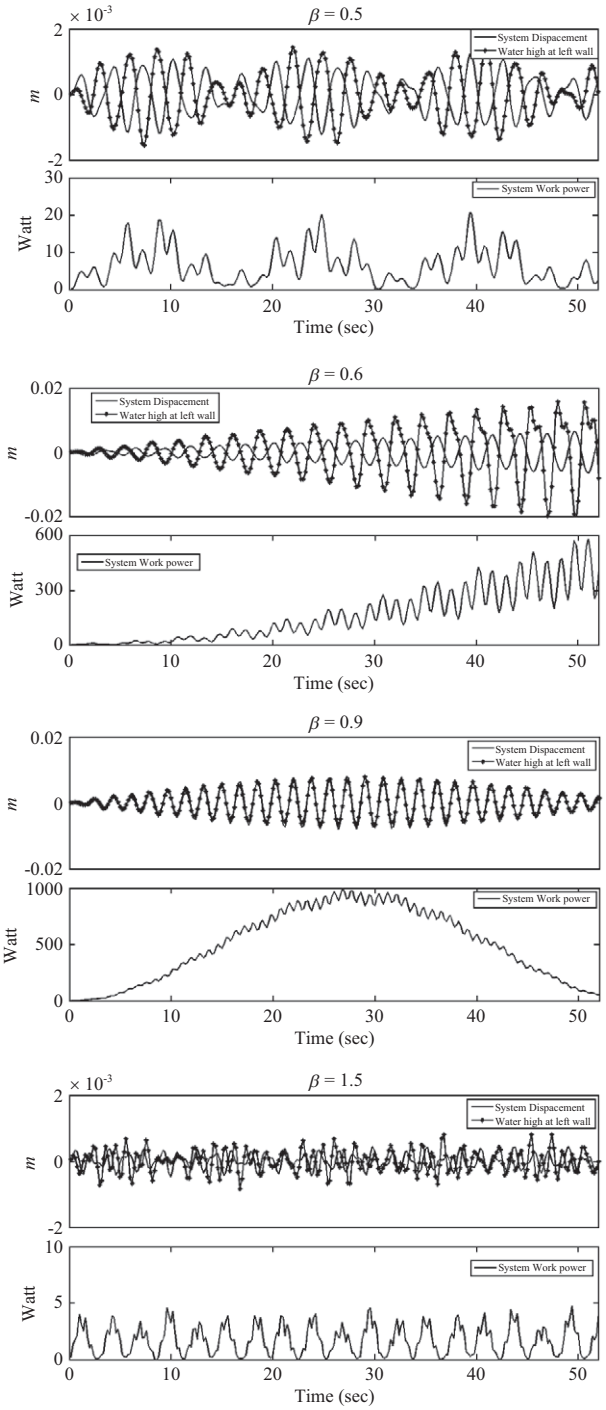

Fig. 12. The time-history of dynamic displacement of structure and water elevation at left wall of tank and the total energy built up in the system under various excitation frequencies.

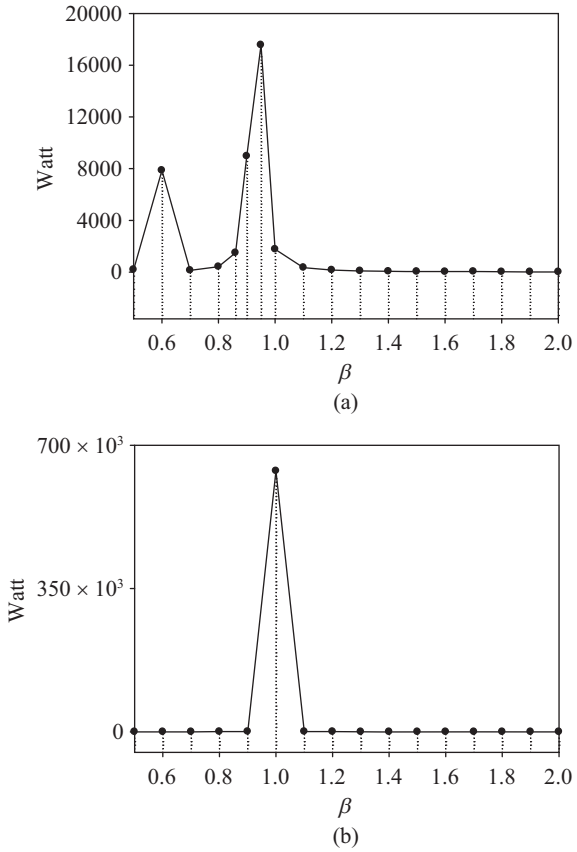

Fig. 13. The maximum energy development in the tank-structure system during various excitation frequencies, μ = 1 / 3 and d_0/b = 0.15.

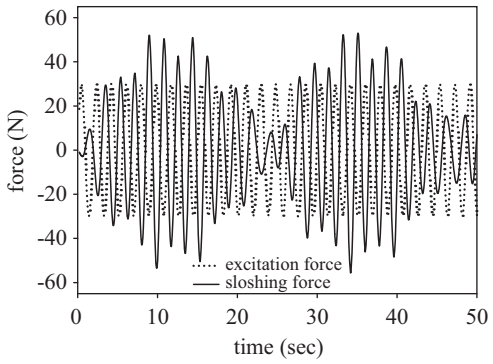

Fig. 14. The time-histories of the sloshing force and excitation force, μ = 1/3, β = 0.86.

The sloshing motion of a fluid resulting from the vibration of the structure dissipates a portion of the energy released by dynamic loading, thus increasing the equivalent damping of the structure. Fig. 14 presents the time histories of the sloshing and excitation forces. The sloshing force is usually equal in magnitude but opposite in direction to the exciting force. Therefore, the damping force of the system is mainly derived from the reverse dynamic pressure of the fluid in the tank.

We investigated the effects of water depth on the maximum dynamic displacement in the tank at various excitation frequencies. Thus, two parameters (β and d_0/b) were used to determine the vibration control of the tank-structure system. Fig. 15 shows the maximum sloshing displacement at the left wall of the tank at various excitation frequencies and various water depths. The corresponding dynamic displacements of the tank-structure system are shown in Fig. 16. The maximum

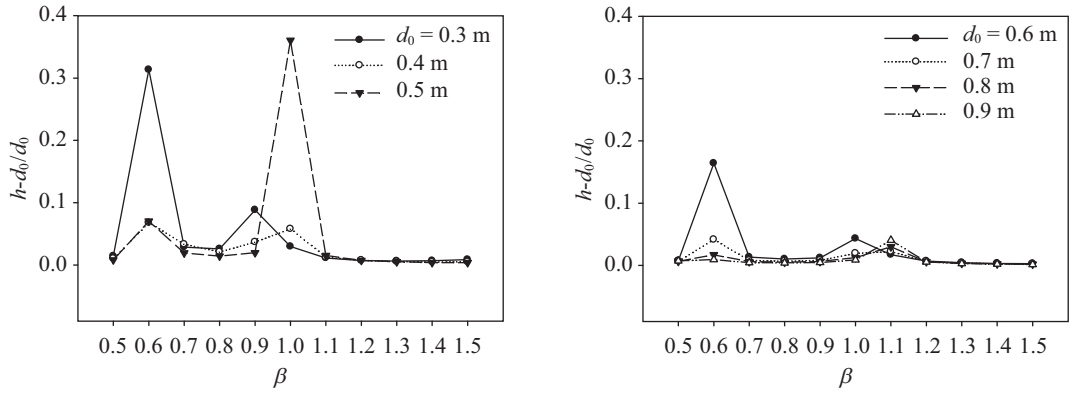

Fig. 15. The maximum sloshing displacement at left wall of the tank under various excitation frequencies and various water depths of the tank, μ = 1/3.

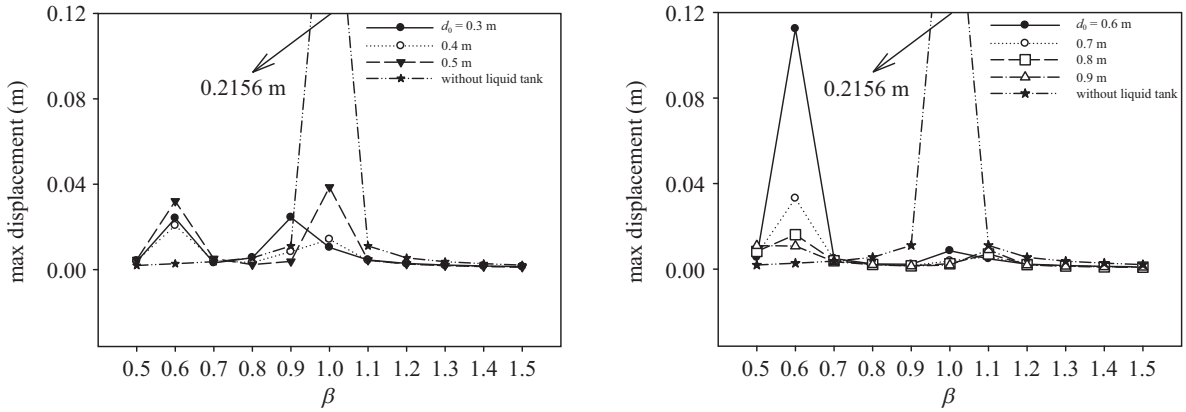

Fig. 16. The dynamic dimensionless displacements of the tank-structure system under various excitation frequencies and various water depths of the tank, μ = 1/3.

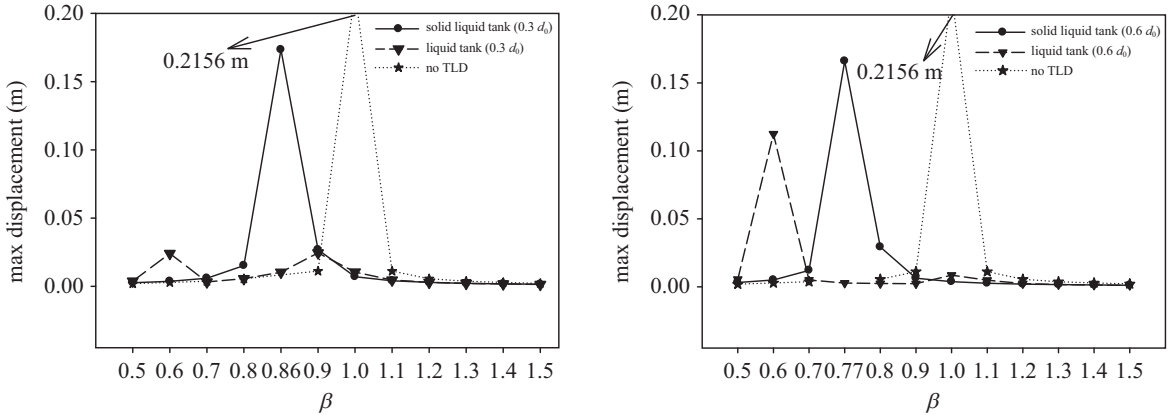

Fig. 17. The comparison of the dynamic dimensionless displacements of the tank-structure system with non-sloshing liquid tank, sloshing liquid tank and without tank, μ = 1 / 3.

sloshing displacements at the left wall showed several prominent peaks corresponding to d_0/b = 0.15, 0.25, and 0.3 at β = 0.6, 1.0, and 0.6, respectively. The intensities of the peaks corresponding at other water depths were considerably lower than those observed for the aforementioned three cases. The dynamic displacement of the structure system exhibited a similar phenomenon. Figs. 15 and 16 provide valuable information the design of a TLD system that can perform appropriate vibration control of a structure. Fig. 17 shows a comparison of the dynamic displacements of various tank-structure systems. The case of a tank without a sloshing liquid reduced the response of the structure. However, the case of a tank with a sloshing fluid has higher reduction of structure displacement.

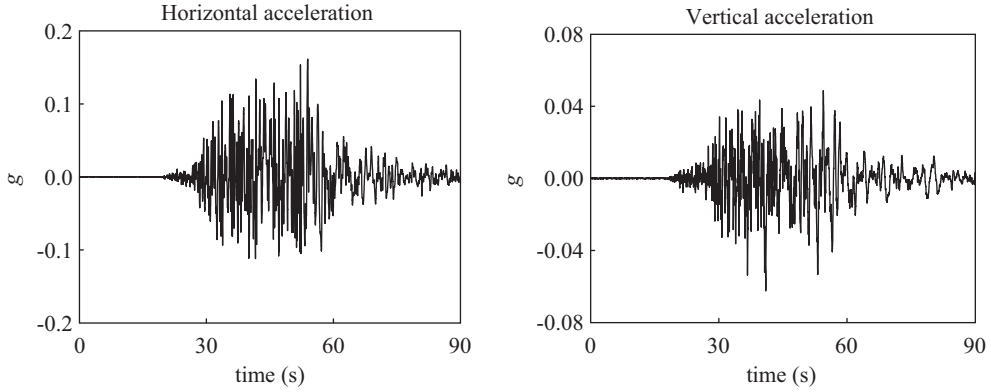

Fig. 18. The time-history of ground acceleration of 1999 Chi-chi Taiwan earthquake (TCU059 station).

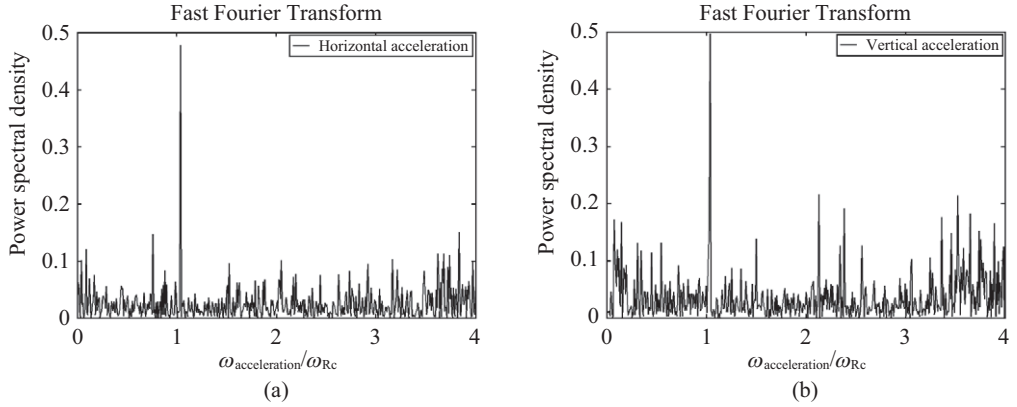

Fig. 19. The FFT analysis of 1999 Chi-chi earthquake (TCU059 station) (a) horizontal ground acceleration, (b) vertical ground acceleration, (the natural frequency of the structure is amended to meet the major frequency of the ground accelerations).

4. Vibration Reduction of a Tank-Structure System in a Real Earthquake Scenario

A tuned liquid tank system can mitigate earthquake- and wind-induced vibrations in tall buildings and long-span bridges. In this section, the 921 Chi-Chi earthquake in Taiwan (station: TCU059) is considered. The time history of the TCU059 record is depicted in Fig. 18. The major frequency components of the ground motions of the 1999 Chi-Chi earthquake were obtained using a fast Fourier transform analysis, and the results are presented in Fig. 19. The natural frequency of the tank-structure system was tuned to meet the major ground acceleration frequency of the 1999 Chi-Chi earthquake, and the excitation was considered a near-resonant excitation.

Fig. 20 shows the dynamic response of the displacement of a structure without a tank mounted on it at the coupled horizontal and vertical excitations of the 1999 Chi-Chi earthquake (TCU059). To reduce the vibration of the structure, a fluid-filled tank was mounted on the structure at the same ground excitations; the corresponding dynamic displacements of the tank-structure system are depicted in Fig. 21. The tank-structure system with a fluid depth of 0.6-0.8 m (d_0/b = 0.3-0.4) effectively reduced the vibration of the dynamic displacement of the system. To determine the optimal fluid depth

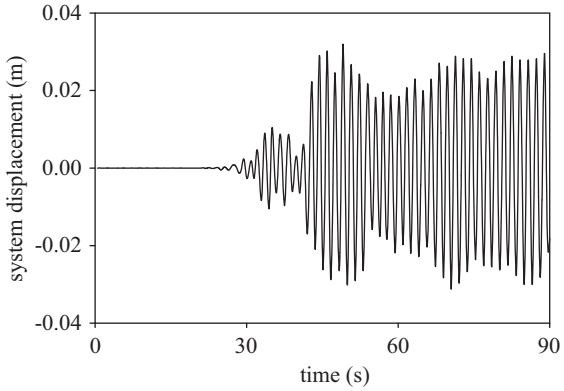

Fig. 20. The dynamic displacement response of base-structure under coupled horizontal and vertical ground accelerations of 1999 Chi-chi earthquake (TCU059 station).

in the tank-structure system, we calculated the maximum energy developed in the system during earthquake excitation. Fig. 22 illustrates the maximum energy developed in the tank-structure system with various fluid depths; the lowest energy was obtained at $d_0/b = 0.35$. The maximum energies of a base structure without a tank mounted on it and a tank-

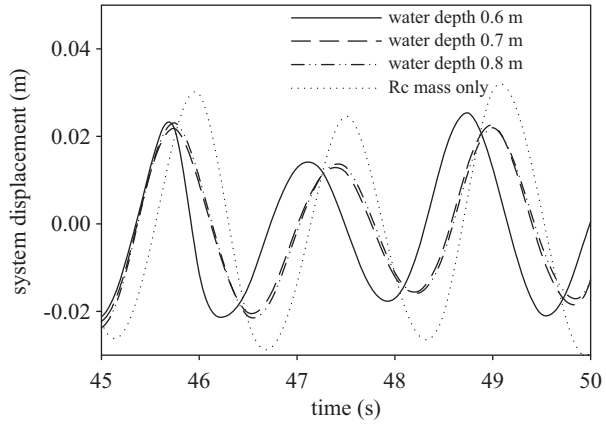

Fig. 21. The dynamic displacement response of tank-base structure system with various fluid depths in tank, the system is under coupled horizontal and vertical ground accelerations of 1999 Chi-chi earthquake (TCU059 station).

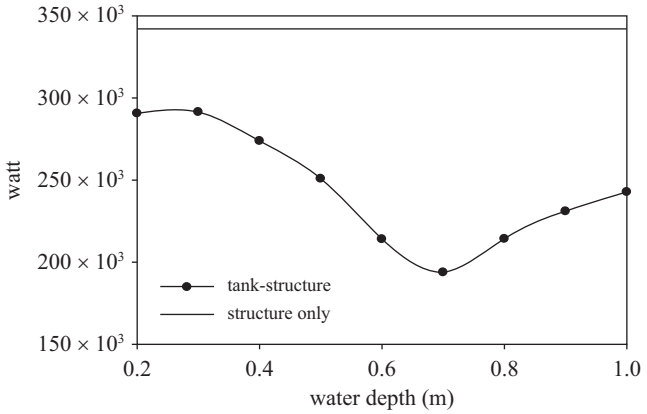

Fig. 22. The maximum energy development in a tank-structure system with various water depths in the tank, μ = 0.01, under 1999 Chi-chi earthquake (TCU059 station).

structure system were 348,000 and 200,000 W, and the tuned tank-structure system with d_0/b = 0.35 significantly reduced the vibration energy of the system. A significant sloshing displacement and energy developed in a tank-structure system effectively reduces the vibration displacement of the system.

IV. CONCLUSION

A time-independent finite difference method (Chen and Nokes, 2005) was used to study the sloshing fluid-structure interaction. The numerical results were validated using several benchmark studies. Vibration control was simulated for both large and small structures, and the following conclusions were derived:

1. For a large structure, an appropriate water depth in the tank significantly reduced the dynamic displacement of the tank-structure system, whereas an inappropriate water depth enhanced the dynamic response of the structure.

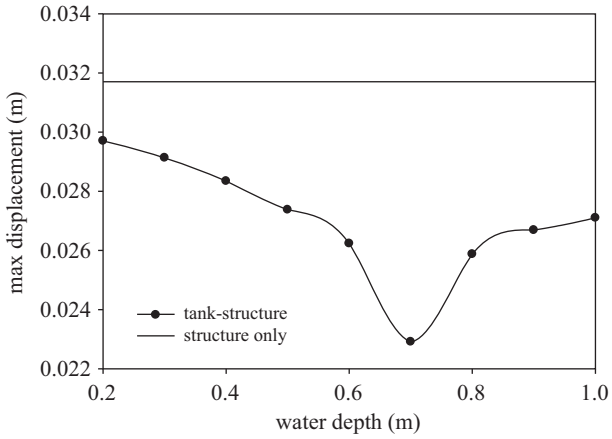

Fig. 23. The maximum displacement of a tank-structure system with various water depths in the tank, μ = 0.01, under 1999 Chi-chi earthquake (TCU059 station).

2. For a small structure, the numerical results revealed that the energy developed in a system was closely related to both the dynamic displacement of the structure and the sloshing displacement of the fluid in the tank. For a fluid-filled tank with water depth = 0.15 b was used, the maximum energy developed in the tank-structure system was only one-tenth that of a structure without a tank mounted on it. The tuned liquid tank can be used for the vibration control of a small structure.
3. The vibration of a structure in a real earthquake scenario was studied. Tuned liquid tanks with d_0/b = 0.3-0.35 exhibited the most superior vibration control performance.
4. The developed model can be easily modified to include the response of the vertical displacement of the system, thus enabling the study of a complete two-dimensional earthquake excitation.

ACKNOWLEDGMENTS

The study was supported by the National Science Council of ROC under grants NSC 97-2221-E-110-087 and NSC 98-3114-P-110-001.

REFERENCE

Armenio, V. and M. L. Rocca (1996). On the analysis of sloshing of water in rectangular containers: numerical study and experimental validation. Ocean Engineering 23(8), 705-739.

Banerji, P., M. Murudi, A. H. Shah and N. Popplewell (2000). Tuned liquid dampers for controlling earthquake response of structures. Earthquake Engineering and Structural Dynamics 29(5), 587-602.

Chen, B. F.(1994). Nonlinear hydrodynamic pressures by earthquakes on dam faces with arbitrary reservoir shapes. J. Hyd. Res. 32(3), 401-413.

Chen, B. F. (1997). 3D nonlinear hydrodynamic analysis of a vertical cylinder during earthquakes, I: Rigid motion. J. Engineering Mechanics 123(5), 458-465.

Chen, B. F. (1999). Viscous free surface effects on coastal embankment hydrodynamics. Ocean Engineering 26, 47-65.

Chen, B. F. and S. W. Chiang (1999). Complete 2D and fully nonlinear

analysis of sloshing fluid in a rigid; ideal fluid. J. Engineering Mechanics 125(1), 70-78.

Chen, B. F. and R. Nokes (2005). Time-independent finite difference analysis of 2D and nonlinear viscous fluid sloshing in a rectangular tank. J. of Computational Physics 209, 47-81.

Faltinsen, O. M. (1978). A numerical non-linear method of sloshing in tanks with two dimensional flow. J. Ship Res. 31(2), 125-135.

Faltinsen, O. M., O. F. Rognebakke and A. N. Timokha (2005). Classification of three-dimensional nonlinear sloshing in a square-base tank with finite depth. J. Fluids Structures 20, 81-103.

Frandsen, Jannette B. (2004). Sloshing motions in excited tanks. Journal of Computational Physics 196, 53-87.

Frandsen, J. B. (2005). Numerical predictions of tuned liquid tank structural systems. Journal of Fluids and Structures 20, 309-329.

Fujino, Y., B. M. Pacheco, P. Chaiseri and L. M. Sun (1988). Parametric studies on tuned liquid damper (tld) using circular containers by free-oscillation experiments. JSCE Journal of Structural Engineering/ Earthquake Engineering 5, 381-391.

Gardarsson, S., H. Yeh and D. Reed (2001). Behavior of sloped-bottom tuned liquid dampers. ASCE Journal of Engineering Mechanics 127, 266-271.

Kim, Y. (2001). Numerical simulation of sloshing flows with impact loads. Applied Ocean Res. 23, 53-62.

Koh, C. G., S. Mahatma and C. M. Wang (1994). Theoretical and experimental studies on rectangular liquid dampers under arbitrary excitations. Earthq. Engrg. Str. Dynam. 23, 17-31.

Kareem, A., T. Kijewski and Y. Tamura (1999). Mitigation of motions of tall buildings with specific examples of recent applications. Journal of Wind and Structures 2, 201-251.

Lepelletier, T. G. and F. Raichlen (1988). Nonlinear oscillations in rectangular tanks. ASCE Journal of Engineering Mechanics 114, 1-23.

Nomura, T. (1994). ALE finite element computations of fluid-structure interaction problems. Computer Methods in Applied Mechanics and Engineering 112, 291-308.

Nakayama, T. and K. Washizu (1981). The boundary element method applied to the analysis of two-dimensional nonlinear sloshing problems. Int. J. Num. Meth. in Eng. 17, 1631-1646.

Okamoto, T. and M. Kawahara (1990). Two-dimensional sloshing analysis by Lagrangian finite element method. Int. J. Num. Meth. Fluids 11, 453-477.

Reed, D., J. Yu, H. Yeh and S. Gardarsson (1998). An investigation of tuned liquid dampers under large amplitude excitation. Journal of Engineering Mechanics, ASCE 124, 405-413.

Sun, L. M., Y. Fujino, B. M. Pacheco and P. Chaiseri (1992). Modeling of tuned liquid damper (TLD). Journal of Wind Engineering and Industrial Aerodynamics 41-44, 1883-1894.

Yamamoto, K. and M. Kawahara (1999). Structural oscillation control using tuned liquid damper. Computers and Structures 71, 435-446.